Structural Investigation of the Charge-transfer Transition in Two-dimensional Cyanide Complex

A charge-transfer (CT) transition that is a cooperative charge-transfer between neighboring molecular units is frequently observed in organic compounds and transition metal complexes, such as halogen-bridged gold complex ($Cs_2Au_2X_6$ (X=I, Br, Cl)) and cyanide complex ($RbMn[Fe(CN)_6]$, $NaCo[Fe(CN)_6] \times H_2O$). The characteristics of the CT transition are that the transition is accompanied by a significant change in the spin state and in the lattice structure. Kato *et al.* have performed electron-level structural analysis of $RbMn[Fe(CN)_6]$, and clarified the variation in the bonding between the Mn ion and the CN ligands [1]. From this viewpoint, the investigation of structural properties, especially the configuration of both metal ions, is indispensable for deeper comprehension of the CT transition as well as of the physical properties.

We chose $Cs[Co(3\text{-}CNpy)_2]W(CN)_8{\cdot}H_2O$(CoW cyanide) with 2-dimensional CoW sheet as the target compound. The compound is stoichiometric and is suitable for precise structural analysis with the maximum entropy method (MEM) analysis. The CoW compound shows the thermally-induced CT transition at T_{CT} = 216 K from the Co3+(S=0)-W4+(S=0) configuration to the Co2+(S=3/2)-W5+(S=1/2) configuration. The same CT transition is further induced by photo-irradiation with visible light (600-750 nm, 12.5 mW/cm^{-2}) at 5 K, which causes photo-induced magnetization [2].

The CoW compound consists of cyano-bridged CoW sheets stacked in the *b* direction. Among the eight CN moieties of the octacyanotungsten $[W(CN)_8]$, four are linked to the neighboring Co atoms to form a zigzag sheet, as shown in Fig. 1.

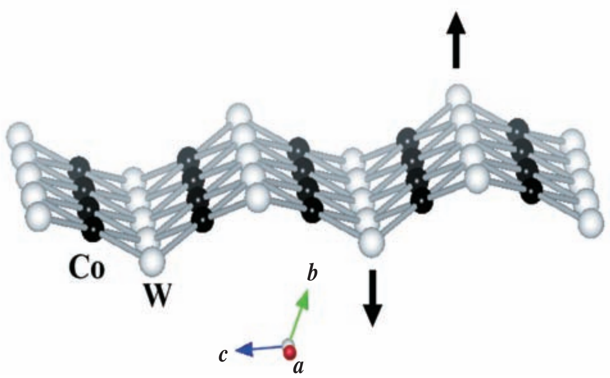

Fig. 1. Cyano-bridged Co-W layer of $Cs[Co(3\text{-}CNpy)_2]W(CN)_8{\cdot}H_2O$. White and black circles represent W and Co, respectively. Arrows indicate the out-of-plane movement of the W atoms.

In order to investigate the structural properties of the CoW compounds in the thermally- and photo-induced CT transitions, we measured the powder X-ray pattern at **BL02B2** beamline. The high-energy X-rays reduce the absorption effect even in CoW compounds. The powder diffraction method is free from the mosaicness, which is inevitably introduced at the first-order CT transition. The experiment was carried out with the large Debye-Scherrer camera in the powder X-ray diffraction beamline BL02B2. The wavelength of the incident X-ray was 0.82866 Å. The powder sample was sealed in a 0.1 mmϕ capillary. The temperature was controlled in the range from 90K to 300K by a cooling system of flowing a nitrogen gas. The exposure time was 5 min (60 min) for the photo-induced phase (HT phase and LT phase). In the photo-excitation measurements, the sample powders were thinly attached to the inner surface of the capillary to enable uniform photo-excitation. The excitation laser was a CW green laser (532 nm)

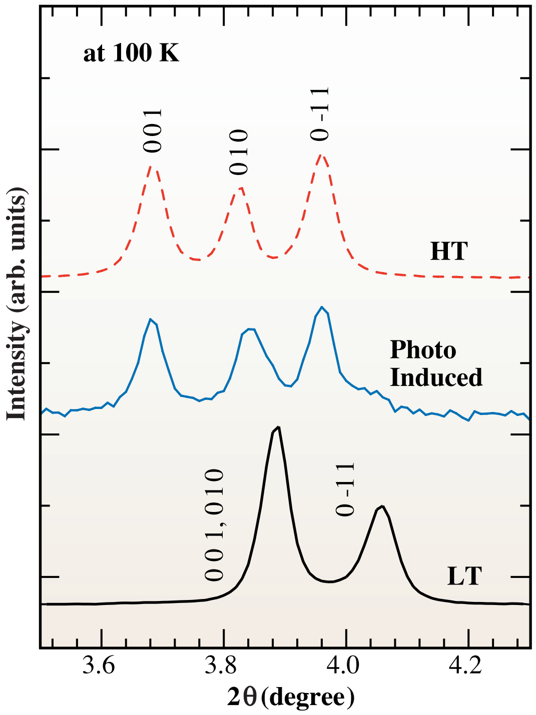

Fig. 2. Magnified X-ray diffraction patterns of $Cs[Co(3\text{-}CNpy)_2]W(CN)_8{\cdot}H_2O$. The wavelength of the X-ray was 0.82866 Å. LT and HT represent the low-temperature phase and high-temperature phase, respectively. The photo-induced phase was obtained after irradiation by a continuous-wave laser (532 nm, 10 mW/mm^2) for 30 min. The exposure time was 5 min (60 min) for the photo-induced phase (HT phase and LT phase).

operating at 50 mW. The laser spot size was 1mmϕ at the capillary. The temperature rise at the photo-excitation was estimated to be 30 K.

Figure 2 shows the X-ray diffraction pattern of the high temperature phase (HT), low temperature phase (LT), and photo-induced (PI) phase obtained at 100K. We have analyzed the HT and LT patterns by the Rietveld analysis with the triclinic (*P*-1, *Z*=2) space group. We analyzed the PI pattern with the two phase model and were not able to refine the atom positions. The obtained cell parameters are listed in Table 1. The lattice parameter *a*(*c*) of the HT phase increased by 3% (5%) over the LT phase, while the angles do not change significantly. We found that the cell parameters of the PI phase are close to those of the HT phase. We conclude that the photo-induced magnetization of the CoW compounds is due to the photo-induced structural change to the HT-like metastable structure.

To investigate the detailed structure changes of HT and LT phases, we list the Co-W bond lengths and the Co-W-Co bond angle in Table 2. At the CT transition, the Co-W bond length elongates by ≈0.21 Å. This elongation shows up as an increase in the cell parameters. Indeed, the *y* coordinate of the W atom in the HT phase increased 5% over the LT phase. Yokoyama *et al*. reported that the distance of Co2+(Co3+)-W is 5.37±0.02(5.15±0.02) by means of X-ray absorption fine structure (XAFS) spectroscopy [3]. This elongation of the Co-W bond is consistent with the value determined in this investigation.

In summary, we have investigated the structural properties at the thermally- and photo-induced CT transitions of $Cs[Co(3\text{-}CNpy)_2]W(CN)_8{\cdot}H_2O$. A charge density-level structural analysis as well as an electrostatic potential analysis [4] is in progress, which will clarify the nature of the CT transition of the CoW compound.

Table 1. The cell parameter with triclinic setting. υ is the cell volume. The reliable factors are defined as

$$R_{wp}=\left[\frac{\sum_i w_i(y_i-u_{i,calc})^2}{\sum_i w_i y_i^2}\right]^{1/2} \quad R_I=\left[\frac{\sum_K \left|I_{K,calc}-I_K\right|}{\sum_K I_{K,calc}}\right]$$

	LT	HT	PI
a (Å)	7.1245(2)	7.3157(2)	7.3067(7)
b (Å)	13.8479(4)	13.9564(4)	13.844(1)
c (Å)	13.6980(4)	14.3791(4)	14.336(1)
α (deg)	116.854(2)	116.223(2)	116.379(8)
β (deg)	90.008(2)	90.010(2)	89.997(6)
γ (deg)	97.702(3)	97.068(3)	96.598(8)
υ ($Å^3$)	1192.00(7)	1304.48(15)	1288.4(2)
R_{wp} (%)	4.57	4.64	2.71
R_I (%)	4.85	5.12	13.86

Table 2. The bond distance and angles in Co-W. The atomic positions, Co1(-1/2, 0, 1/2), Co2(-1/2,0,0), and W(x,y,z) are also shown

$d_{Co1\text{-}W}$(Å)	5.136(2)	5.334(2)
$d_{Co1\text{-}W}$(Å)	5.160(2)	5.372(2)
$d_{Co2\text{-}W}$(Å)	5.151(2)	5.354(3)
$d_{Co2\text{-}W}$(Å)	5.175(2)	5.390(3)
average(Å)	5.155(2)	5.362(3)
$\theta_{Co1\text{-}W\text{-}Co2}$(deg)	146.85(6)	146.01(6)
x	0.0338(3)	0.0334(4)
y	0.1204(1)	0.1264(2)
z	0.3058(2)	0.3052(2)

J. E. Kim [a,*] and Y. Moritomo [b]

[a] SPring-8 / JASRI
[b] Department of Physics, University of Tsukuba

*E-mail: kimj@spring8.or.jp

References

[1] K. Kato *et al.*: Phys. Rev. Lett. **91** (2003) 255502.
[2] Y. Arimoto *et al.*: J. Am. Chem. Soc. **125** (2003) 9240.
[3] T. Yokoyama *et al.*: Phys. Rev. B **65** (2002) 064438.
[4] H. Tanaka *et al.*: Phys. Rev. B **74** (2006) 172105.
[5] *J.E. Kim and Y. Moritomo et al.: Phys. Rev. B **76** (2007) 172105.*